PHILOSOPHICAL TRANSACTIONS OF THE ROYAL SOCIETY B BIOLOGICAL SCIENCES

The Aerodynamics of Hovering Insect Flight. I. The Quasi-Steady Analysis

C. P. Ellington

Phil. Trans. R. Soc. Lond. B 1984 **305**, 1-15
doi: 10.1098/rstb.1984.0049

Phil. Trans. R. Soc. Lond. B **305**, 1–15 (1984)

Printed in Great Britain

THE AERODYNAMICS OF HOVERING INSECT FLIGHT. I. THE QUASI-STEADY ANALYSIS

By C. P. ELLINGTON

Department of Zoology, University of Cambridge, Downing Street, Cambridge CB2 3EJ, U.K.

(*Communicated by Sir James Lighthill, F.R.S.* – *Received* 28 *March* 1983)

CONTENTS

The conventional aerodynamic analysis of flapping animal flight invokes the 'quasi-steady assumption' to reduce a problem in dynamics to a succession of static conditions: it is assumed that the instantaneous forces on a flapping wing are equivalent to those for steady motion at the same instantaneous velocity and angle of attack. The validity of this assumption and the importance of unsteady aerodynamic effects have long been controversial topics. Weis-Fogh tested the assumption for hovering animal flight, where unsteady effects are most pronounced, and concluded that most insects indeed hover according to the principles of quasi-steady aerodynamics. The logical basis for his conclusion is reviewed in this paper, and it is shown that the available evidence remains ambiguous.

The aerodynamics of hovering insect flight are re-examined in this series of six papers, and a conclusion opposite to Weis-Fogh's is tentatively reached. New morphological and kinematic data for a variety of insects are presented in papers II and III, respectively. Paper IV offers an aerodynamic interpretation of the wing kinematics and a discussion on the possible roles of different aerodynamic mechanisms. A generalized vortex theory of hovering flight is derived in paper V, and provides a method of estimating the mean lift, induced power and induced velocity for unsteady as well as quasi-steady flight mechanisms. The new data, aerodynamic mechanisms and vortex theory are all combined in paper VI for an analysis of the lift and power requirements and other mechanical aspects of hovering flight.

Vol. 305 B 1122. 1 [Published 24 February 1984

A large number of symbols are needed for the morphological, kinematic and aerodynamic analyses. Most of them appear in more than one paper of the series, and so a single comprehensive table defining the major symbols from all of the papers is presented at the end of this paper.

1. Introduction

Research into the aerodynamic principles of flapping animal flight has long been hampered by a limited repertoire of investigative tools. Aerodynamics is primarily a practical science, concentrating on the forces experienced by a wing in steady motion. The effects of periodic variations in wing attitude and velocity superimposed on a mean motion have been investigated in flutter analysis, but such analytical treatments employ linearizations that restrict them to small amplitude oscillations. The scope for theoretical analyses of animal flight has thus been severely limited, and from necessity it is generally assumed that the instantaneous forces on a flapping wing are those corresponding to steady motion at the same instantaneous velocity and attitude, the *quasi-steady assumption*. Whether or not this assumption is valid for large amplitude, high frequency motions has been the source of much controversy, and a decisive test can only be accomplished by comparing measured instantaneous wing forces with those predicted by the assumption. The aerodynamic characteristics of a wing in steady motion are easily determined, but a direct measurement of the cyclic forces produced by flapping animal wings has only been achieved recently (Cloupeau *et al.* 1979; Buckholtz 1981), and a comprehensive test of the assumption using these difficult techniques is still lacking. Researchers have therefore been forced to adopt a debatable assumption which could not be tested experimentally.

The validity of the quasi-steady explanation of flapping flight can be tested theoretically only in a proof-by-contradiction. The mean forces generated by the wings during a cycle are calculated according to the quasi-steady assumption. If these forces do not satisfy the net force balance of the flying animal, then the assumption must be false. If the mean quasi-steady forces do satisfy the balance, then the only logical conclusion is that the assumption cannot be discounted. The range of forces generated by wings is restricted by physical considerations: unconventional aerodynamic mechanisms may produce mean, and even instantaneous, forces very similar to the quasi-steady values. A satisfactory explanation of flight based on the quasi-steady assumption cannot preclude alternative mechanisms.

The early quantitative studies on the aerodynamics of flapping flight have been reviewed by Weis-Fogh & Jensen (1956). The available data on wing motion, the *kinematics*, were incomplete and often inaccurate, so it was usually necessary to base the theories on rough kinematic approximations. Some studies concluded that the wing forces were not consistent with a quasi-steady mechanism, but the sources of error were too large for an unqualified acceptance of the conclusions. In a classic series of papers Weis-Fogh and Jensen then presented what is still the most complete study of flapping flight for the desert locust *Schistocerca gregaria*. The kinematics of fast forward flight and the aerodynamic characteristics of the wings in steady motion were measured (Weis-Fogh 1956; Jensen 1956). Jensen (1956) then combined these data in a quasi-steady analysis and found that the mean calculated wing forces agreed well with those measured from locusts flying in a wind tunnel. This is a very persuasive argument for the quasi-steady explanation of fast forward flight, but it cannot be considered as a proof. Indeed, the cyclic force measurements of Cloupeau *et al.* (1979) on *Schistocerca* indicate that the quasi-steady mechanism is not a sufficient explanation in this case.

PHILOSOPHICAL TRANSACTIONS OF THE ROYAL SOCIETY B BIOLOGICAL SCIENCES

It is generally believed that the quasi-steady assumption is valid for fast forward flight because of the low value of the reduced frequency parameter. This parameter, the ratio of a flapping velocity of the wings to the forward flight velocity, may be expressed in several ways and was introduced to animal flight studies by Walker (1925). At low values, the steady flight velocity dominates the flow over the wings and reduces the spatial derivatives of the fluctuating aerodynamic parameters. Thus unsteady aerodynamic effects are small compared with quasi-steady ones.

At slower flight speeds the reduced frequency parameter increases and unsteady effects should become more important. Hovering flight presents the extreme condition where the flight velocity is zero and the reduced frequency becomes infinite. Bennett (1966) and Weis-Fogh (1972, 1973) emphasized the increased significance of unsteady effects to be found in hovering flight. The wings accelerate and decelerate in a distance of only a few chord lengths: virtual mass forces and unsteady circulatory effects may no longer be negligible. The amplitude of wing rotation about a longitudinal axis during pronation and supination exceeds a right angle, and the rotational velocity is comparable with the flapping velocity. Under these conditions the aerodynamic behaviour of the wings may differ appreciably from the quasi-steady assumption. By exaggerating the unsteady aerodynamic effects of flapping flight, hovering thus presents an ideal case for the investigation of flight mechanisms.

In addition to its advantage in stressing unsteady effects, a study of hovering is useful from other considerations. The force and moment balance during flight is simplified by the lack of a net horizontal thrust, and the effects of body lift and body drag can be ignored. The absence of a linear flight velocity acting in combination with the flapping velocity also reduces the complexity of the mathematical treatment. Excluding brisk manoeuvres and climbing flight, the lift coefficients of the wings during hovering must be greater than other types of flight because the relative velocity of the wings is not enhanced by the flight velocity. Thus hovering demands maximum lift coefficients, which are particularly useful when comparing the wing performance with steady-state conditions. Finally, the total power expenditure of the animal is greatest in hovering flight, providing a convenient case for physiological discussions.

Weis-Fogh (1972, 1973) applied a quasi-steady analysis to hovering animal flight and concluded that 'most insects perform normal hovering on the basis of the well-established principles of steady-state flow' (Weis-Fogh 1973). The aerodynamics of hovering flight are re-examined in this study using new data and a new theory, and the opposite conclusion is strongly indicated. Before this work is presented, the previous approaches to the problem will be reviewed.

2. The blade-element theory

The usual aerodynamic treatment of animal flight is based on the *blade-element theory* of propellers developed by Drzewiecki. Osborne (1951) derived the general equations that apply to flapping flight. The fundamental unit of the analysis is the blade element, or wing element, which is that portion of a wing between the radial distances r and $r+\mathrm{d}r$ from the wing base (figure 1*a*). The aerodynamic force F' on a wing element can be resolved into a component normal to the flow velocity, called the lift, and a component parallel to the flow, called the profile drag (figure 1*b*). The lift L' and profile drag D'_{pro} for a wing section of spanwise width $\mathrm{d}r$ are

$$L' = \tfrac{1}{2}\rho c U_{\mathrm{r}}^2 C_{\mathrm{L}}, \tag{1}$$

$$D'_{\mathrm{pro}} = \tfrac{1}{2}\rho c U_{\mathrm{r}}^2 C_{\mathrm{D,\,pro}}, \tag{2}$$

PHILOSOPHICAL TRANSACTIONS OF THE ROYAL SOCIETY B BIOLOGICAL SCIENCES

where ρ is the mass density of air, c is the wing chord, and U_r is the relative velocity component perpendicular to the longitudinal wing axis. Any spanwise component of the relative velocity is assumed to have no effect on these forces. C_L and $C_{D,pro}$ are lift and profile drag coefficients, which can be defined for unsteady as well as steady motion. According to the quasi-steady assumption, though, these coefficients are functions only of the Reynolds number and angle of attack of the relative wind for given profile characteristics. Equations (1) and (2) are resolved into vertical and horizontal components, integrated along the wing length and averaged over a cycle. For hovering flight the net force balance requires the mean vertical force to equal the weight of the animal, and the mean horizontal force to be zero.

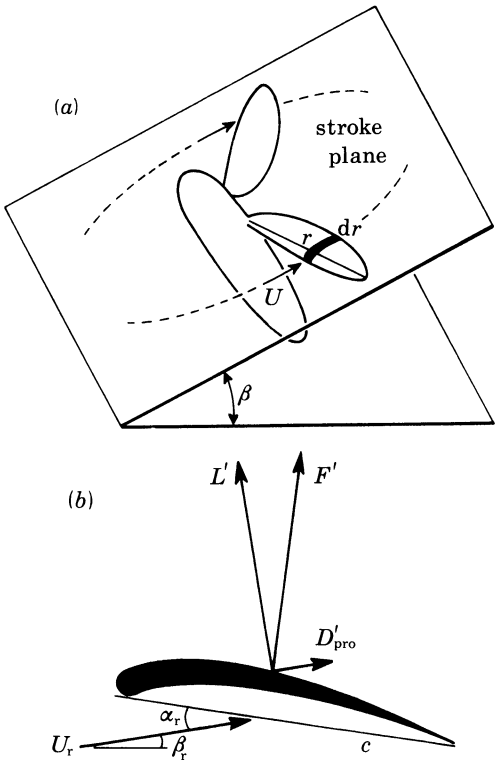

FIGURE 1. (*a*) The wingbeat during hovering is approximately confined to a stroke plane, which is inclined at an angle β to the horizontal. The aerodynamic parameters for a wing element of width dr and chord c are shown in a two-dimensional view in (*b*).

The relative velocity is the vector sum of the flapping velocity U and the induced velocities of bound and wake vorticity. The blade-element theory ignores the existence of vortices, however, and so can reveal nothing of the induced velocity. Following Osborne (1951), a mean value of the vertical induced velocity w_0 is usually estimated by the Rankine–Froude axial momentum theory of propellers.

One method of applying the blade-element analysis relies on successive stepwise solutions of equations (1) and (2). Complete kinematic data are necessary for this approach: the motion of the longitudinal wing axis, the geometrical angle of attack and the section profile must all be known as functions of time and radial position. The angle of attack of the relative wind α_r can then be calculated, and appropriate values of C_L and $C_{D,pro}$ selected from experimental

measurements. This was the method used so effectively by Jensen (1956) in his study of forward flight in the desert locust, but it becomes increasingly unreliable as the hovering state is approached, where momentum considerations show that the wake induced velocity reaches a maximum. For many hovering animals there are periods when the opposite wings are separated by a distance of less than a chord length, so that the bound vorticity of the opposite wing will also contribute significantly to the relative velocity of a wing. This effect can only be approximated and, when coupled with the crude estimate of the wake induced velocity, a considerable inaccuracy can be expected for the calculated value of α_r. The lift coefficient is strongly dependent on α_r, so the solution to equation (1) is prone to serious error.

Osborne (1951) introduced an alternative method of analysis which solves for mean values of the coefficients, $\overline{C_L}$ and $\overline{C_{D,\,pro}}$, satisfying the net force balance. This is equivalent to assuming that the force coefficients are constant along the wing and throughout the cycle. The assumption is not unreasonable, because the wings could well be operating at some optimal angle of attack. For small insects like *Drosophila*, C_L is nearly constant anyway over the range of α_r found during flight (Vogel 1967). The mean lift coefficient is particularly interesting because it is also the *minimum* value compatible with flight; if C_L varies during the wing beat then some instantaneous values must exceed $\overline{C_L}$. The kinematic detail required for this method is greatly reduced since only the motion of the longitudinal wing axis is needed. The geometrical angle of attack and profile section of the wings are extremely difficult to measure accurately, and one of the principal advantages of this method is its neglect of them. The double integrals of radius and time produced by manipulation of equations (1) and (2) can be separated when the coefficients are assumed to be constant; the resulting single integrals may then be reduced to morphological and kinematic parameters, allowing simple expressions to be derived for $\overline{C_L}$ and $\overline{C_{D,\,pro}}$ satisfying the integral constraints.

The theoretical investigations of hovering flight have usually relied on the mean coefficients method (Weis-Fogh 1972, 1973; Ellington 1975; R. Å. Norberg 1975; U. M. Norberg 1975, 1976). The animals studied so far can be divided into three functional groups, for which different approximations can be used in the calculations outlined above. During a cycle the wings beat roughly in a *stroke plane*, which is inclined at an angle β with respect to the horizontal (figure 1*a*); it is the attitude of this stroke plane that distinguishes the groups.

3. Kinematic groups

3.1. *Horizontal stroke plane*

The most commonly observed type of hovering is characterized by an approximately horizontal stroke plane (figure 2*a*). This group was extensively discussed by Weis-Fogh (1972, 1973), who called the pattern *normal hovering*, and includes the hummingbirds (Stolpe & Zimmer 1939; Greenewalt 1960) and most insects (Weis-Fogh 1973). The amplitude of wing rotation during pronation and supination is large, enabling the wings to operate at an angle of attack favourable for lift on both the morphological downstroke and the upstroke (figure 2*a*, *b*). The wake induced velocity is small with respect to the flapping velocity of the wings for this group, resulting in a relative velocity very close to the horizontal (Ellington 1978, 1980). This justifies using the horizontal flapping velocity for U_r in equation (1) and neglecting any small drag contributions to the net vertical force. A mean lift coefficient is then easily found such that the

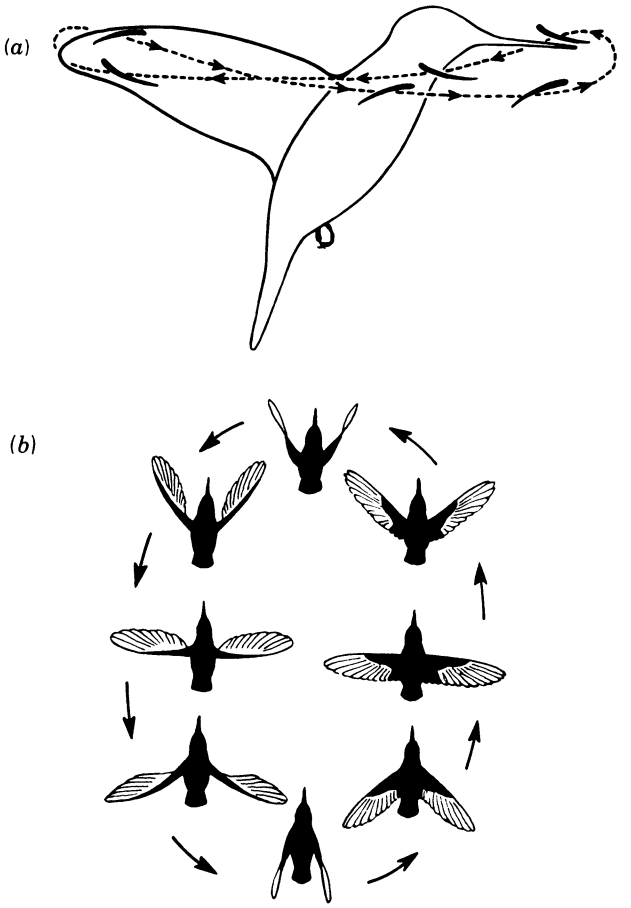

FIGURE 2. (*a*). The wing tip path of a hummingbird *Chlorostilbon aureoventris* viewed from the side, illustrating a horizontal stroke plane. The wing attitude is indicated on the path. (*b*) The wingbeat pattern for *Melanotrochilus fuscus* viewed from above. Adapted from Stolpe & Zimmer (1939).

net lift given by the integral form of equation (1) balances the body mass. A mean drag coefficient cannot be determined by the integral constraints, but once $\overline{C_L}$ is calculated an appropriate $\overline{C_{D,pro}}$ may be selected from experimental measurements.

In his comparative survey of normal hovering animals, Weis-Fogh (1973) used simple analytical expressions for wing chord and flapping velocity; a semi-elliptical wing planform was used, and the flapping velocity was taken as simple harmonic motion. These are reasonable approximations, permitting a quick calculation of $\overline{C_L}$, but increase the error to an estimated 30%. Table 1 presents some of Weis-Fogh's results and a Reynolds number *Re* for the wings; the Reynolds number is based on the chord and the mean flapping velocity at 0.7 of the wing length. $\overline{C_L}$ for the small wasp *Encarsia formosa* is taken from Ellington (1975). In this case the wing shape and velocity were not well represented by Weis-Fogh's approximations and a more detailed treatment was necessary.

3.2. *Inclined stroke plane*

Small passerine birds (Zimmer 1943; Brown 1963; U. M. Norberg 1975), bats (Eisentraut 1936; U. M. Norberg 1970, 1976) and the 'true' hover-flies of the subfamily Syrphinae

(Weis-Fogh 1973) hover with the stroke plane inclined at a value of β between 30° and 40° (figure 3). Dragonflies (Odonata) also hover in this manner, although β is about 60° (R. Å. Norberg 1975). These animals appear to generate relatively small forces on the upstroke. The dragonfly *Aeschna juncea* strongly supinates its wings on the upstroke, making the angle of attack near zero (R. Å. Norberg 1975). Excluding the hummingbirds, vertebrate fliers are anatomically unable to rotate their wings to this extent. The birds and bats partially flex their wings during the upstroke, however, and the individual primaries of birds are also rotated to a negligible angle of attack. Any lift on the upstroke of an inclined stroke plane would produce a large horizontal thrust component, and this is probably the explanation for insignificant upstroke lift. The mean force on the downstroke is thus primarily responsible for mass support.

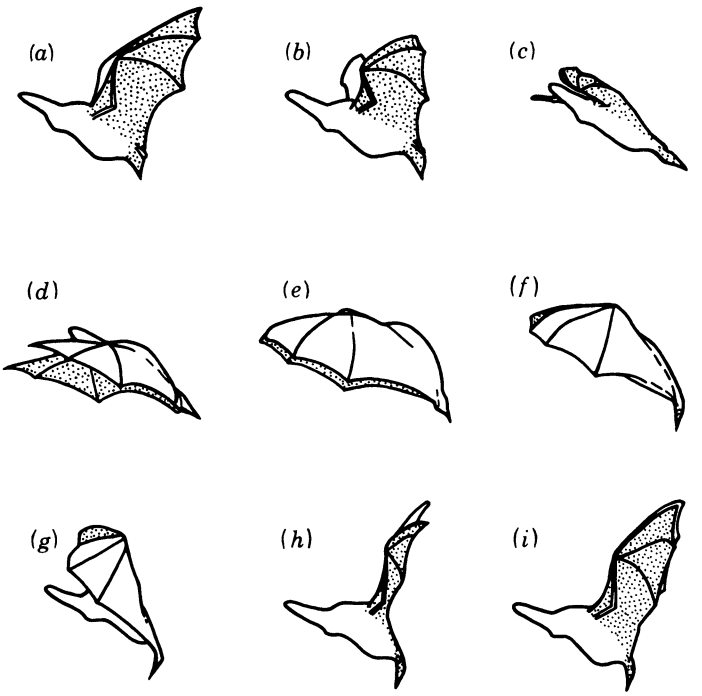

FIGURE 3. The wingbeat of the long-eared bat *Plecotus auritus*, illustrating an inclined stroke plane during hovering flight. Adapted from U. M. Norberg (1970).

The relative velocity U_r on the downstroke should not be approximated by the flapping velocity; because of the inclination of the stroke plane, the induced velocity will reduce the value of U_r^2 well below U^2. An accurate estimate of the induced velocity is therefore essential in calculating the magnitude and direction of the relative velocity. It is likely that previous estimates of the induced velocity are substantially too small (see papers V and VI), which led to an incorrect consideration of downstroke profile drag by Ellington (1980). From the results of R. Å. Norberg (1975) and estimates based on papers V and VI, the value of $\overline{C_L}$ required for weight support on the downstroke of *Aeschna juncea* should lie between 3 and 4. U. M. Norberg (1975) calculated that $\overline{C_L}$ must equal 5.3 for the net vertical force on the downstroke to balance the body mass of the pied flycatcher *Ficedula hypoleuca*. In paper VI, I estimate that $\overline{C_L}$ for *Ficedula* is about 6.0, so a value between 5 and 6 can be expected. It should be noted that in both cases the morphological and kinematic data were not from the same animals, and so an unknown inaccuracy is present.

The effects of different assumptions about upstroke forces on the mean coefficients were evaluated by U. M. Norberg (1976) in a thorough investigation of hovering in the bat *Plecotus auritus*. Her results demonstrate that minimum coefficients occur when no lift is generated on the upstroke, which then requires $\overline{C_L} = 3.1$ on the downstroke; my estimate of $\overline{C_L}$ is about 4.3 (paper VI), and so a value between 3 and 4 seems probable. She also commented on Weis-Fogh's (1973) analysis of *Plecotus*, noting that his procedural simplifications were invalid. This is also true of his calculations for other animals using an inclined or vertical stroke plane.

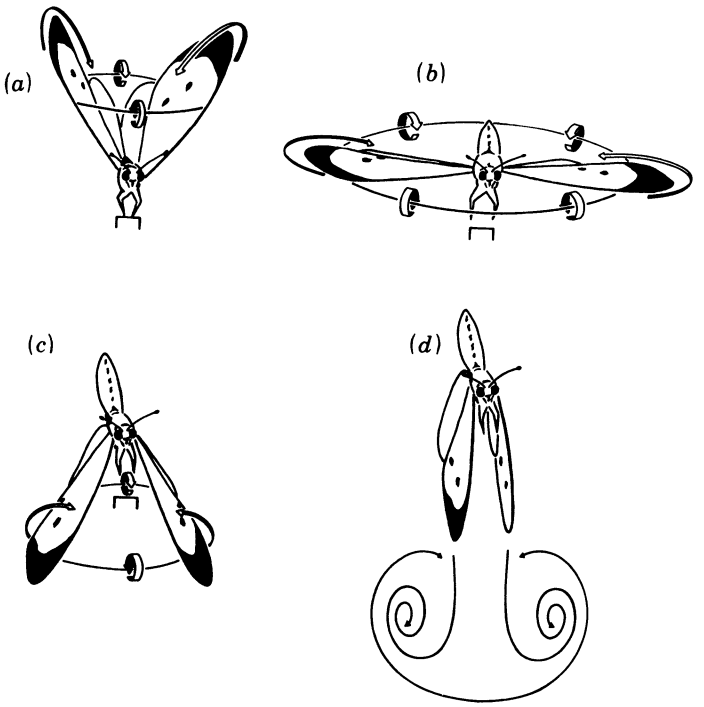

FIGURE 4. The downstroke of a vertical take-off by *Pieris brassicae*. The stroke plane is vertical, and the wing motion is perpendicular to the chord. The vortex pattern created by the downstroke is indicated, and the resulting large-cored vortex ring is shown in vertical section in (*d*).

3.3. *Vertical stroke plane*

In addition to the insects covered in paper III, I have filmed the Large Cabbage White butterfly *Pieris brassicae* L. in free flight. A unique kinematic pattern, an approximately vertical stroke plane, is often seen during take-off and hovering. Figure 4 shows several stages of the downstroke which initiates a vertical take-off from a small platform. The wings are clapped together dorsally at the start of the downstroke, and then 'fling' open (Weis-Fogh 1973) as in figure 4*a*. The wings move with the chord perpendicular to their motion (figure 4*b*, *c*) and nearly clap together at the end of the downstroke (figure 4*d*). The body pitches nose-up and the wings strongly supinate during the upstroke, which is not shown here, producing an angle of attack near zero. Thus little force is generated on the upstroke, as for the inclined stroke plane.

The sustaining vertical force obviously results from the pressure drag on the wings during the downstroke. A drag mechanism of flight has been suggested several times for flight at Reynolds numbers below about 100 (Horridge 1956; R. Å. Norberg 1972*a*, *b*; Bennett 1973),

where thick boundary layers reduce the steady-state lift coefficients of wings. The drag is mainly due to skin friction at low *Re*, however, and is not very sensitive to α_r. A drag mechanism based on a differential velocity of the half-strokes was therefore proposed (Bennett 1973), such that the downstroke velocity and drag were greater than the upstroke. However, the small wasp *Encarsia* was found to use a horizontal stroke plane and a circulatory lift mechanism (Weis-Fogh 1973; Lighthill 1973; Ellington 1975). I have also filmed the small fringe-winged insect *Thrips physapus* and the fruit fly *Drosophila melanogaster* (Ellington 1983); the kinematics and aerodynamics are very similar to *Encarsia*. Ironically the drag mechanism does not operate for small insects, for which it was predicted, but rather for a large one at higher Reynolds number (about 2800). The pressure drag during the downstroke is much greater than the skin friction drag of the upstroke at high *Re*, and so the need for a velocity differential is eliminated.

TABLE 1. RESULTS FROM THE QUASI-STEADY ANALYSIS

(References: 1, Weis-Fogh (1972); 2, Weis-Fogh (1973); 3, Ellington (1975); 4, R. Å. Norberg (1975); 5, U. M. Norberg (1975); 6, U. M. Norberg (1976); 7, present study.)

species	$\overline{C_L}$	*Re*	ref.
horizontal stroke plane			
Amazilia fimbriata fluviatilis	1.8	6100	(1)
Melolontha vulgaris	0.6	3900	(2)
Manduca sexta	1.2	5400	(2)
Bombus terrestris	1.2	3600	(2)
Apis mellifera	0.8	1600	(2)
Eristalis tenax	0.9	1600	(2)
Tipula sp.	0.8	630	(2)
Drosophila virilis	0.8	210	(1)
Encarsia formosa	1.6	23	(3)
inclined stroke plane			
Plecotus auritus	3–4	15000	(6,7)
Ficedula hypoleuca	5–6	11000	(5,7)
Aeschna juncea	3–4	1900	(4,7)
vertical stroke plane			
Pieris brassicae	0	2800	(7)

Equation (2) of the blade-element analysis could be applied to the Large Cabbage White butterfly, but a constant value of $C_{D,pro}$ on the downstroke is unlikely because of pressure interference from the opposite wings. A different aerodynamic approach has been developed, therefore, based on the vortex pattern created by the wing motion. Air rushes into the gap between the wings as they fling open at the beginning of the downstroke, producing a sink motion bounded by the vorticity on the wing surfaces and the free vortex lines connecting the leading edges and the trailing edges (figure 4*a*). This flow pattern is maintained and strengthened during the downstroke, resulting in a large-core vortex ring (figure 4*d*). The reaction force and kinetic energy associated with this ring have been estimated from flow visualization photographs. Although this flight mechanism is conceptually quite simple, many subtle modifications to the flow are effected by wing twisting and flexibility, and a detailed analysis will be presented elsewhere (Ellington 1983).

PHILOSOPHICAL TRANSACTIONS OF THE ROYAL SOCIETY B BIOLOGICAL SCIENCES

4. The proof-by-contradiction

The mean lift coefficient has been chosen in all of the hovering analyses to test the quasi-steady assumption. If $\overline{C_L}$ is greater than the maximum steady-state lift coefficient $C_{L,\,max}$, then the assumption is contradicted and unsteady flight mechanisms must be invoked. When $\overline{C_L}$ is about equal to $C_{L,\,max}$ the test is not conclusive: some variation of the lift coefficient is likely during a cycle, and instantaneous values may then exceed the mean.

Values of $C_{L,\,max}$ are not known for the animals in table 1. For the insects we may note a value of 1.1 at *Re* about 2000 for the flat forewing of a desert locust, which rises to 1.3 when the vannal region is depressed as a flap (Jensen 1956). Nachtigall (1977) measured a smaller $C_{L,\,max}$ of 0.85, however, for a crane-fly (*Tipula oleracea*) wing at a similar *Re* of 1500. Vogel (1967) found a value of 0.6 for a flat *Drosophila virilis* wing at a lower *Re* of 200, which increases to 0.8 for a cambered wing; his results are very similar to those of Thom & Swart (1940) for a flat-bottomed aerofoil in this low *Re* range. Of the insects in table 1, *Encarsia* and *Aeschna* are the only examples where $\overline{C_L}$ definitely exceeds $C_{L,\,max}$ for the relevant *Re*, and unsteady effects are therefore indicated. The flight mechanism of *Pieris* has already been outlined and must also be considered as unsteady. Values of $\overline{C_L}$ for the remaining insects are uncomfortably close in general to the expected values of $C_{L,\,max}$, and several lie in the region of uncertainty between Jensen's and Nachtigall's results. Because of this and the large margin of error in Weis-Fogh's (1973) analysis, no firm conclusions can be drawn concerning these insects.

The values of $C_{L,\,max}$ for bird and bat wings are more controversial than those for insects. The wings are thin and highly cambered, and generally operate at *Re* between 10^4 and 10^5. Experiments on similar aerofoil sections have found $C_{L,\,max}$ up to 1.6; a very strong camber or an effective increase in camber resulting from leading edge and trailing edge flaps can raise the value to about 2.5 (Schmitz 1957; Abbott & Doenhoff 1959; Mises 1959; Tucker & Parrott 1970; Hoerner & Borst 1975). Which of these sections best respresents avian and bat wings is not clear. Primary separation on the downstroke of birds may function as slotted or multi-slotted flaps (Graham 1932), which can produce values of $C_{L,\,max}$ in excess of 3. The alula of bird wings is commonly raised in slow and hovering flight, increasing the lift some 25% by acting as a Handley–Page leading edge slot (Nachtigall & Kempf 1971). These comparisons indicate that $C_{L,\,max}$ may be about 1.6 for the wings, and possibly much more.

Measurements on bird wings and wing models suggest that these values are too high. Even with the alula raised, $C_{L,\,max}$ for the wing of a house sparrow *Passer domesticus* is only 1.1 at *Re* 16000, and for a European blackbird *Turdus merula* it is only 0.8 at *Re* 24000 (Nachtigall & Kempf 1971). Measurements from many other bird wings over an *Re* range of 10000–50000 are much the same: 0.7–1.2 (Withers 1981). There are problems of course, to mounting a wing in a realistic attitude in a wind tunnel. Studies on wing models of the pigeon *Columba livia* show a similar range of values, however, from 0.8 to 1.2 (Nachtigall 1979). For gliding birds and bats values around 1.5 are found for the maximum lift coefficient based on wing area (Pennycuick 1968, 1971; Tucker & Parrott 1970), but when the tail area is included as a lifting surface $C_{L,\,max}$ drops to about 1.3 for the pigeon (Pennycuick 1968). The values of $C_{L,\,max}$ actually measured for bird wings and wing models are thus well below those that might be expected.

For the hummingbird $\overline{C_L}$ is 1.8, which Weis-Fogh (1973) accepted as possible under quasi-steady conditions. Judging by the results above, I think that this is unlikely and unsteady

PHILOSOPHICAL TRANSACTIONS OF THE ROYAL SOCIETY B BIOLOGICAL SCIENCES

effects will then be significant. For *Plecotus* $\overline{C_L}$ is 3–4, which should be greater than $C_{L,\max}$ for a bat wing. The quasi-steady assumption fails for *Ficedula* as well.

The results of the analysis can now be summarized for the kinematic groups. The animals using an inclined or vertical stroke plane rely on unsteady flight mechanisms, as concluded by Weis-Fogh (1973); the quasi-steady mechanism is insufficient even as an approximation to the aerodynamic forces. Of the animals using a horizontal stroke plane, *Encarsia* must use an unsteady mechanism, and this is probably true for the hummingbird as well. The proof is not conclusive for the remaining animals, but their values of $\overline{C_L}$ are very close to $C_{L,\max}$.

From such results Weis-Fogh (1973) concluded that most animals hovering with a horizontal stroke plane rely on the quasi-steady flight mechanism. However, three points must be borne in mind when interpreting these results. If $\overline{C_L}$ does not exceed $C_{L,\max}$, then the proof-by-contradiction only demonstrates that the quasi-steady assumption cannot be discounted; it does not prove that the assumption is true. Furthermore, some instantaneous values of the lift coefficient are likely to be greater than the mean $\overline{C_L}$ over the cycle. And finally, the mean lift in unsteady motion can be substantially smaller than the quasi-steady estimate because of the Wagner effect, so the wings cannot actually achieve the maximum lift during hovering that is predicted by $C_{L,\max}$ (paper IV). In the light of these last two points, the close agreement between $\overline{C_L}$ and $C_{L,\max}$ *could* indicate that the quasi-steady mechanism is *not* able to provide sufficient lift for hovering. The example of the hummingbird could also lead to a conclusion contrary to Weis-Fogh's. The kinematics of most insects are similar to those of the hummingbird, and it would be surprising if different flight mechanisms were involved; if the quasi-steady explanation is indeed inadequate for the hummingbird, then it might not apply to the insects either. Much more research is obviously required before Weis-Fogh's conclusion can be substantiated or disproved.

5. Outline of the present study

The aerodynamics of hovering insect flight are re-examined in this series of papers, to evaluate the roles of quasi-steady and unsteady aerodynamic mechanisms. Any aerodynamic study must be based on accurate kinematic and morphological data, and the previous studies have usually been unsatisfactory in this respect: the amplitude of wing motion was often determined only by visual estimation, some of the data used by Weis-Fogh (1973) were from insects in slow forward flight, and the morphological and kinematic data were not from the same animals in the analyses of *Aeschna*, *Ficedula* and *Amazilia*. Papers II and III present complete data sets for a variety of insects to be used in this study.

Weis-Fogh (1973) proposed two unsteady flight mechanisms for animals where the quasi-steady assumption fails, based on an aerodynamic interpretation of the wing kinematics. This approach is followed in paper IV to discuss the possible roles of different aerodynamic mechanisms.

The flight mechanisms considered in paper IV cannot be directly incorporated into the blade-element theory. A more generalized vortex theory is therefore developed in paper V, which calculates the mean lift for unsteady as well as quasi-steady mechanisms. The theory also provides more accurate estimates for the induced velocity and induced power than previously possible.

The new flight data, aerodynamic mechanisms and vortex theory are all combined in paper

VI for an analysis of the flight mechanisms, their power requirements, and other mechanical considerations of hovering flight.

This study would not have been possible without the help, encouragement and guidance of three men: the late Professor T. Weis-Fogh, who inspired the initial lines of research, Dr K. E. Machin, whose many talents and enthusiastic support were vital to the fruition of much work, and Mr G. G. Runnalls, whose photographic expertise was invaluable. To these three, I extend my warmest gratitude.

6. Symbol table

This table contains all of the major symbols in this series of papers. Except for a few general symbols, the paper where each symbol is defined is given below. Some symbols are defined formally by equations, and this is indicated by XX.xx, where XX is the paper number and xx is the equation number within that paper. A 'hat' denotes a non-dimensional form of a symbol. Other modifications to symbols obey the following rules unless a special definition is presented below: subscripts 'max' and 'min' refer to maximum and minimum values, a bar over the symbol indicates a time-averaged mean value, a prime denotes a force per unit span, and an asterisk represents mechanical power per unit body mass.

symbol	paper or equation no.	definition
a	V	axial separation of vortex rings in the far wake
A	V	cross-sectional area of the far wake
A_0	V.10	area of the actuator disc
A_r	V	area of the vortex sheet produced by a half-stroke
A'_r	V	rolled-up area of that vortex sheet
$\mathcal{R}$	II.4	aspect ratio of the wing pair
b	V	radius of vortex rings in the far wake
b_0	V	radius of vortex rings at the actuator disc
c	II	chord of the wing
$\bar{c}$	II.5	mean chord
$\hat{c}$	II	$c/\bar{c}$
C	V.34	self-induced component of the vortex ring velocity
C_D		drag coefficient
$C_{D,f}$	IV.7	C_D for a flat plate parallel to the flow
$C_{D,pro}$		profile drag coefficient
C_L		lift coefficient
$\hat{d}$	II.17	mean diameter of body/body length
d/u	III	ratio of duration of downstroke to upstroke
$\bar{D}$	VI	magnitude of the mean profile drag vector
$\hat{D}$	VI.32	$\bar{D}/mg$
D_{pro}		profile drag
f	V	frequency of lift impulses
$\hat{f}$	VI	f/wingbeat frequency
F		aerodynamic force on a wing
or		
F	V	the force from a momentum jet
g		gravitational acceleration
$\hat{h}$	II.11	mean wing thickness/wing length
I	V	circulatory lift impulse
$\hat{I}$	V.5	non-dimensional form of I
I_0	V	the impulse required for weight support
or		
I	II	moment of inertia
I_b	II	moment of inertia for animal body
I_v	II	moment of inertia for the virtual mass of a wing pair
I_w	II	moment of inertia for the mass of a wing pair

PHILOSOPHICAL TRANSACTIONS OF THE ROYAL SOCIETY B BIOLOGICAL SCIENCES

J	III.23	advance ratio
k	V.31	specific induced power factor
K	V.33	component of the vortex ring velocity due to other rings in the wake
$\hat{l}$	II.18	distance from anterior end of body to centre of mass/body length
$\hat{l}_1$	II	distance from forewing base axis to centre of body mass/body length
$\hat{l}_2$	II.20	radius of gyration for the body/body length
L	II	body length
$\hat{L}$	II	body length/wing length
or		
L		lift
$\bar{L}$	VI	mean lift/mg
m		body mass
m_w	II	mass of wing pair
$\hat{m}_w$	II	m_w/m
m_k	II.8	the kth moment of wing mass about the wing base
n		wingbeat frequency
p_d	V	disc loading
p_w		wing loading
P_a	VI	aerodynamic power
P_{acc}	VI.39	power required to accelerate mass and virtual mass of the wings
P_{ind}	VI.20	induced power
P_m	VI	mechanical power output of muscle
$\overline{P_m^*}$	VI	$\bar{P}_m$ per unit weight of muscle
P_{pro}	VI.29	profile power
P_{RF}	VI.21	Rankine–Froude estimate of induced power
r		radial position along the wing
$\hat{r}$		r/wing length
$\hat{r}_k(m)$	II.9	non-dimensional radius of the kth moment of wing mass
$\hat{r}_k(S)$	II.7	non-dimensional radius of the kth moment of wing area
$\hat{r}_k(v)$	II.16	non-dimensional radius of the kth moment of virtual mass
R		wing length
Re	VI.28	Reynolds number
s	V.36	spacing parameter
S	II.3	wing area
S_k	II.6	kth moment of wing area
t		time
$\hat{t}$		t/wingbeat period
U		flapping velocity of the wing
U_r	V.8	relative velocity of the wing
U_t	III	flapping velocity of the wing tip
v	V	axial velocity of vortex ring
or		
v	II.13	virtual mass of a wing pair
$\hat{v}$	II.14	non-dimensional virtual mass of a wing pair
v_k	II.15	kth moment of virtual mass
V	III	flight velocity
$\hat{V}$	III	V/nR = number of wing lengths travelled per wingbeat
w	V	axial wake velocity in the far wake
w_0	V	axial wake velocity at the actuator disc = induced velocity
w_{RF}	V	Rankine–Froude estimate of w
$w_{0,RF}$	V	Rankine–Froude estimate of w_0
x_0	IV	distance from leading edge to axis of wing rotation
$\hat{x}_0$	IV	x_0/c
α	IV	geometrical angle of attack
α'	IV	angle of incidence
α_0	IV	zero-lift angle of attack
α_r	IV	effective angle of attack
α'_r	IV	effective angle of incidence
β	IV	half-angle between chords during fling
or		
β		stroke plane angle
β_0	III	value of β in 'true' hovering
β_r	VI.4	relative stroke plane angle

PHILOSOPHICAL TRANSACTIONS OF THE ROYAL SOCIETY B BIOLOGICAL SCIENCES

γ	VI.13	rotational lift coefficient
Γ		circulation
$\hat{\Gamma}$	V	non-dimensional circulation ($=\Gamma/\Gamma_{\max}$)
$\bar{\hat{\Gamma}}$	V	mean of $\hat{\Gamma}$ over area of vortex sheet
$\bar{\hat{\Gamma}}^{\frac{3}{2}}$	V	mean of $\hat{\Gamma}^{\frac{3}{2}}$ over area of vortex sheet
Γ_0	V	circulation of a pulsed Froude actuator disc
δ	VI.34	magnitude of the mean profile drag/mean of the magnitude of the profile drag
ϵ	IV.14	downwash angle
or		
ϵ	V	core radius of vortex ring in far wake
ϵ_0	V	core radius of vortex ring at actuator disc
η	III	roll angle
η_a	VI.53	aerodynamic efficiency
θ	III.22	angle of elevation of wing with respect to stroke plane
λ	IV	distance travelled by wing element/chord
Λ	IV.17	value of λ over a half-stroke
$\bar{\Lambda}$	IV.18	mean distance travelled by wing over a half-stroke/mean chord
ν		kinematic viscosity of air
ξ	III	angle between mean flight path and the horizontal
ρ		mass density of air
ρ_b	II	mass density of the body
ρ_w	II	mass density of the wing
σ	V.43	spatial correction factor for induced power
τ	V.44	temporal correction factor for induced power
ϕ		positional angle of wing in the stroke plane
$\hat{\phi}$	III.24	non-dimensional form of ϕ
Φ		stroke angle
χ	III	angle between longitudinal body axis and the horizontal
χ_0	III	free body angle
ω	III	angular velocity during pronation and supination
$\dot{\omega}$	III	mean angular velocity/wingbeat frequency

References

Abbott, I. H. & Doenhoff, A. E. von 1959 *Theory of wing sections*. New York: Dover

Bennett, L. 1966 Insect aerodynamics: vertical sustaining force in near-hovering flight. *Science, N.Y.* **152**, 1263–1266.

Bennett, L. 1973 Effectiveness and flight of small insects. *Ann. ent. Soc. Am.* **66**, 1187–1190.

Brown, R. H. J. 1963 The flight of birds. *Biol. Rev.* **38**, 460–489.

Buckholtz, R. H. 1981 Measurements of unsteady periodic forces generated by the blowfly flying in a wind tunnel. *J. exp. Biol.* **90**, 163–173.

Cloupeau, M., Devilliers, J. F. & Devezeaux, D. 1979 Direct measurements of instantaneous lift in desert locust; comparison with Jensen's experiments on detached wings. *J. exp. Biol.* **80**, 1–15.

Eisentraut, M. 1936 Beitrag zur Mechanik des Fledermausfluges. *Z. wiss. Zool.* **148**, 159–188.

Ellington, C. P. 1975 Non-steady-state aerodynamics of the flight of *Encarsia formosa*. In *Swimming and flying in Nature* (ed. T. Y. Wu, C. J. Brokaw & C. Brennen), vol. 2, pp. 783–796. New York: Plenum Press.

Ellington, C. P. 1978 The aerodynamics of normal hovering flight: three approaches. In *Comparative physiology – water, ions and fluid mechanics* (ed. K. Schmidt-Nielsen, L. Bolis & S. H. P. Maddrell), pp. 327–345. Cambridge University Press.

Ellington, C. P. 1980 Vortices and hovering flight. In *Instationäre Effekte an schwingenden Tierflügeln* (ed. W. Nachtigall), pp. 64–101. Wiesbaden: Franz Steiner.

Ellington, C. P. 1983 Paper in preparation.

Graham, R. R. 1932 Slots in the wings of birds. *Jl R. aeronaut. Soc.* **36**, 598–600.

Greenewalt, C. H. 1960 *Hummingbirds*. New York: Doubleday.

Hoerner, S. F. & Borst, H. V. 1975 *Fluid-dynamic lift*. Bricktown, New Jersey: Hoerner Fluid Dynamics.

Horridge, G. A. 1956 The flight of very small insects. *Nature, Lond.* **178**, 1334–1335.

Jensen, M. 1956 Biology and physics of locust flight. III. The aerodynamics of locust flight. *Phil. Trans. R. Soc. Lond.* B **239**, 511–552.

Lighthill, M. J. 1973 On the Weis-Fogh mechanism of lift generation. *J. Fluid Mech.* **60**, 1–17.

Mises, R. von 1959 *Theory of flight*. New York: Dover.

Nachtigall, W. 1977 Die aerodynamische Polare des Tipula-Flügels und eine Einrichtung zur halbautomatischen Polarenaufnahme. In *The physiology of movement; biomechanics* (ed. W. Nachtigall), pp. 347–352. Stuttgart: Fischer.

PHILOSOPHICAL TRANSACTIONS OF THE ROYAL SOCIETY B BIOLOGICAL SCIENCES

Nachtigall, W. 1979 Der Taubenflügel in Gleitflugstellung: Geometrische Kenngrössen der Flügelprofile und Luftkrafterzeugung. *J. Orn., Lpz.* **120**, 30–40.
Nachtigall, W. & Kempf, B. 1971 Vergleichende Untersuchungen zur Flugbiologischen Funktion des Daumenfittichs (*Alula spuria*) bei Vögeln. *Z. vergl. Physiol.* **71**, 326–341.
Norberg, R. Å. 1972*a* Flight characteristics of two plume moths, *Alucita pentadactyla* L. and *Orneodes hexadactyla* L. (Microlepidoptera). *Zool. Scr.* **1**, 241–246.
Norberg, R. Å 1972*b* Evolution of flight of insects. *Zool. Scr.* **1**, 247–250.
Norberg, R. Å. 1975 Hovering flight of the dragonfly *Aeschna juncea* L., kinematics and aerodynamics. In *Swimming and flying in Nature* (ed. T. Y. Wu, C. J. Brokaw & C. Brennen), vol. 2, pp. 763–781. New York: Plenum Press.
Norberg, U. M. 1970 Hovering flight of *Plecotus auritus* L. *Bijdr. Dierk* **40**, 62–66. (Proc. 2nd int. Bat Res. Conf.)
Norberg, U. M. 1975 Hovering flight of the pied flycatcher (*Ficedula hypoleuca*). In *Swimming and flying in Nature* (ed. T. Y. Wu, C. J. Brokaw & C. Brennen), vol. 2, pp. 869–881. New York: Plenum Press.
Norberg, U. M. 1976 Aerodynamics of hovering flight in the long-eared bat *Plecotus auritus*. *J. exp. Biol.* **65**, 459–470.
Osborne, M. F. M. 1951 Aerodynamics of flapping flight with application to insects. *J. exp. Biol.* **28**, 221–245.
Pennycuick, C. J. 1968 A wind-tunnel study of gliding flight in the pigeon *Columba livia*. *J. exp. Biol.* **49**, 509–526.
Pennycuick, C. J. 1971 Gliding flight of the dog-faced bat *Rousettus aegyptiacus* observed in a wind-tunnel. *J. exp. Biol.* **55**, 833–845.
Schmitz, F. W. 1957 *Aerodynamik des Flugmodells*. Duisburg: Carl Lange Verlag.
Stolpe, M. & Zimmer, K. 1939 Der Schwirrflug des Kolibri im Zeitlupenfilm. *J. Orn., Lpz.* **87**, 136–155.
Thom, A. & Swart, P. 1940 The forces on an aerofoil at very low speeds. *Jl R. aeronaut. Soc.* **44**, 761–770.
Tucker, V. A. & Parrott, G. C. 1970 Aerodynamics of gliding flight in a falcon and other birds. *J. exp. Biol.* **52**, 345–367.
Vogel, S. 1967 Flight in *Drosophila*. III. Aerodynamic characteristics of fly wings and wing models. *J. exp. Biol.* **46**, 431–443.
Walker, G. T. 1925 The flapping flight of birds. *Jl R. aeronaut. Soc.* **29**, 590–594.
Weis-Fogh, T. 1956 Biology and physics of locust flight. II. Flight performance of the desert locust (*Schistocerca gregaria*). *Phil. Trans. R. Soc. Lond.* B **239**, 459–510.
Weis-Fogh, T. 1972 Energetics of hovering flight in hummingbirds and in Drosophila. *J. exp. Biol.* **56**, 79–104.
Weis-Fogh, T. 1973 Quick estimates of flight fitness in hovering animals, including novel mechanisms for lift production. *J. exp. Biol.* **59**, 169–230.
Weis-Fogh, T. & Jensen, M. 1956 Biology and physics of locust flight. I. Basic principles in insect flight. A critical review. *Phil. Trans. R. Soc. Lond.* B **239**, 415–458.
Withers, P. C. 1981 An aerodynamic analysis of bird wings as fixed aerofoils. *J. exp. Biol.* **90**, 143–162.
Zimmer, K. 1943 Der Flug des Nektarvogels (*Cinnyris*). *J. Orn., Lpz.* **91**, 371–387.

PHILOSOPHICAL TRANSACTIONS OF THE ROYAL SOCIETY B BIOLOGICAL SCIENCES